RSC Advances

ROYAL SOCIETY OF CHEMISTRY

www.rsc.org/advances

Journal Name

ARTICLE

Mesenchymal stem cells in response to exposed rod-heights of TiO_2 nanorod films

Received 00th January 20xx,
Accepted 00th January 20xx

DOI: 10.1039/x0xx00000x

www.rsc.org/

Fei Ge[a1], Mengfei Yu[b1], Jun Lin[b], Cuixia Yu[a], Wenjian Wen g[a,c,*], Kui Cheng[a], Huiming Wang[b*]

Cellular responses are strongly sensitive to surface structure, optimizations in the structures are essential in biomaterial research. In this work, the exposed nanorod-heights in TiO_2 nanorod films were adjusted for enhancing cellular responses. The adjustment was realized by incorporating mesoporous bioactive glass (MBG) into the nanorod films via sol-gel method. The exposed nanorod-heights in the films could be changed from original ~300 nm to ~200 nm and ~100 nm. The cellular responses on the nanostructured surfaces were evaluated through culturing mesenchymal stem cells (MSCs). The results showed that the films with shortened nanorod-heights had better cellular responses and could accelerate osteogenic differentiation and mineralization, and the films with 100 nm nanorod-height demonstrated to provide a best surface for cell growth. This is attributed to that the nanostructure with the shortened nanorod-heights could be well recognized by the cells, consequently the cells grew with a faster osteogenic differentiation through a strengthened BMP-smads signal pathway.

1. Introduction

Enhancing interactions of cells with metal implants is crucial to accelerate interfacial bone formation or osseointegration, surface modifications of metal implants through nanostructure is frequently adopted, because surface nanostructures can strongly regulate cell growth, differentiation and bone formation[1-7]. Since nanostructures are usually assembled by geometrical units, such as nanodots, nanofibrous, nanosheets, nanocores, nanotubes and nanorods[4, 8-15], the selection and organization of the geometrical units are closely related to promotion of biological responses[16, 17].

TiO_2 has been extensively used for biomedical purposes in surface nanostructured modification due to its excellence in biocompatibility and versatility as geometrical units, such as TiO_2 nanodots[15], nanowires[16,17], nanotubes[18-2118], and nanorods[22, 23]. The TiO_2 topological structures derived from these units are proved to have obvious and positive influences on cellular behaviours, leading to the enhanced bone forming ability. TiO_2 nanodots-based surfaces could support strong protein adsorption and better cellular responses[9, 15]. The TiO_2 nanotubes-based surface also emerged to enhance cellular growth and accelerate osteogenic differentiation of mesenchymal stem cells (MSCs)[19, 20], which possessing multilineage differentiation capability[16, 19, 20].

Among the various types of TiO_2 nanostructures, there is a particular interest in films obtained by TiO_2 nanorods as geometrical units, because its surface topography has a pseudo-three-dimension surface structure dependent on the nanorod size and density, and could provide a more appropriate microenvironment for cell growth. In our previous work, we changed the nanorod density or made a discontinuous coverage by calcium phosphate, the resulting TiO_2 nanorod films showed significant influence on promoting cellular response and enhancing osteogenic differentiation[24, 25].

In this work, we followed our resent result that the exposed TiO_2 nanorod-height was adjusted by incorporating mesoporous bioactive glass (MBG) into the nanorod films[26], trying to understand cellular responses to changes in the nanorod-height. Mesoporous bioactive glass (MBG) possesses significantly improved specific surface area, pore volume, and apatite mineralization activity due to its well-ordered mesoporous structure. Previously, MBG has been incorporated into bioceramic scaffolds and polymer scaffolds[27-29] to significantly improve their osteogenic activity. The nanostructure of the films was observed by scanning electronic microscope, and cellular responses on the nanostructured surfaces were evaluated through culturing mesenchymal stem cells (MSCs) and assessing their adhesion, proliferation and osteogenic differentiation. The possible biological role of TiO_2 nanorod-height was proposed.

2. Materials and Methods

2.1 Preparation of TiO_2 nanorod films with different nanorod-heights

[a] School of Materials Science and Engineering, State Key Laboratory of Silicon Materials, Zhejiang University, Hangzhou 310027, China.
[b] The First Affiliated Hospital of Medical College, Zhejiang University, Hangzhou 310003, China.
[c] The Shanghai Institute of Ceramics, Chinese Academy of Sciences, Shanghai, 200050, China.
* Corresponding author. Tel. and Fax : +86 571 87953787, Email address: wengwj@zju.edu and chengkui@zju.edu.cn.
1 Contributed equally.

The formation of TiO_2 nanorod films with different nanorod-heights included two steps, preparation of TiO_2 nanorod films and incorporation of MBG. The preparation of TiO_2 nanorod films was described in detail as our previous work[21]. Briefly, TiO_2 nanodot films as crystalline seed layers were firstly prepared on tantalum (Ta) substrates through the phase-separation-induced self-assembly method[22], then hydrothermal treatment was followed to grow nanorods which formed TiO_2 nanorod films.

MBG composition was set as Si/Ca/P/Ti=80/5/5/10 (molar ratio). In synthesis process, the amphiphilic triblock copolymer poly (ethylene glycol)-block-poly (propylene glycol)-block-poly (ethylene glycol) (P123, Mr=5800, Sigma-Aldrich) as the template, and HCl as the catalyst were mixed with ethanol (molar ratio of P123/HCl/ethanol = 0.014/1/30). Afterwards tetraethyl orthosilicate (Aladdin, AR), calcium nitrate tetrahydrate (Aladdin, AR), triethyl phosphate (Aladdin, AR), tetrabutyl tianate (Aladdin, AR) were added according to the set molar ratio, the concentration of TEOS was 0.4 M. After mixing, the sols were stirred for 24 h, and aged in a desiccator containing supersaturated sodium chloride at bottom (T: 4 °C, RH: 75.7 %) for 24 h. And another precursor sol with TEOS concentration of 0.32 M was prepared by increasing amount of ethanol.

The incorporation of MBG was prepared via sol-gel spinning. The precursor sol (20 μL) was dropped onto TiO_2 nanorod films, and then spun at 7000 r/min for 30 s. The resulting substrates were isolated in a desiccator containing supersaturated sodium chloride at bottom (T: 4 °C, RH: 75.7 %) to age for 24 h. After that, the substrates were heated from room temperature to 400 °C at a heating rate of 1 °C /min, and kept at 400 °C for 5 h to remove the residual water and organic moieties. When cooled to the room temperature, they were rinsed extensively with deionized water, and allowed to dry in the air. The two sols resulted in two kinds of exposed TiO_2 nanorod height. As a control, MBG film on Ta was prepared in the same procedure using the sol with TEOS concentration of 0.4 M.

2.2 Characterization

The morphologies of the resulting films were observed via field-emission scanning electron microscopy (FE-SEM, Hitachi, SU-70) and the single nanorod from the film was analysed in chemical element by transmission electron microscopy (TEM, tecnai G2 F20 S-TWIN). To make TEM specimens, the single nanorod containing suspension was obtained by immersing the film into a vial with ethanol and treating under ultrasonication for a few minutes, the suspension was dropped onto carbon-coated 200 mesh copper grids and dried under ambient conditions.

Water contact angle measurement (Dataphysics, OCA20) was performed to characterize the wettability of the films. The water droplets delivered on each sample were set as 1 μL.

2.3 Culture of cells

Bone marrow-derived mesenchymal stem cells (MSCs) were harvested from the femur and tibias of 4-week-old male Sprague-Dawley rats following an established protocol[23]. The third passage of MSCs was used to examine in vitro cellular responses on different films. The cells were cultured with alpha-modified Minimum Essential Medium (α-MEM, Gibco) supplemented with 10 % fetal bovine serum (PAA, Australia), 1 % antibiotic solution containing 10^4 units/mL penicillin and 10 g/L streptomycin (Gibco), 1 % sodium pyruvate (Gibco), and 1 % MEM non-essential amino acids (Gibco) at 37 °C under a humidified 5 % CO_2 atmosphere[24]. Subconfluent MSCs growing on tissue culture polystyrene were trypsinized with 0.25 % trypsin, 1 mM Ethylene Diamine Tetraacetic Acid (Gibco), and were subcultured on different surfaces. The protocol and all experimentation were performed in accordance with the guidelines for animal care established by the Animal Research Committee of Zhejiang University, Hangzhou, China.

2.4 Morphology of cells

The initial attachment morphology of cells was observed by FE-SEM (3 kV of operating voltage). After incubation for 24 h, the culture medium was removed and the cells were fixed in 2.5 % glutaraldehyde overnight at 4 °C. Then, the cells were dehydrated through a series of solution with increasing ethanol concentrations, dried by using a critical point dryer (Hitachi Model Hcp-2) with liquid CO_2, and sputter-coated with gold.

2.5 Cell Counting Kit-8 (CCK-8) assay

Cellular adhesion and proliferation were evaluated by measuring the amount of the cells attached to the films after incubation for 24 hours and 3 days. A cell suspension with a density of 5×10^4 cells/cm^2 was inoculated into a 24-well plate containing the films (500 μL for every well). After designed time intervals, the films were transferred to another 24-well plate after washing 3 times with phosphate-buffered saline (PBS). The CCK-8 (Dojindo Laboratories, Kumamoto, Japan) assay was used to evaluate the relative activity as compared to a control condition (the cells cultured in the absence of films), and the optical density (OD) was measured on a microplate reader at 450 nm.

2.6 Alkaline phosphatase (ALP) activity

The ALP activities of the cells cultured on the films for 7 days and 14 days under a humidified atmosphere of 5 % CO_2 at 37 °C were assayed. The proteins inside the cells were harvested by cell lysisbuffer (9803, Cell Signaling), and they were separated by sodium dodecyl sulfate polyacrylamide gel electrophoresis (SDS-PAGE) on 5 % Tris-HCl reducing gels, ALP

(ab65834, abcam) expression was assessed by the ALP Kit (Beyotime Institute of Biotechnology, Shanghai, China).

2.7 Gene expression analysis

Total RNA was extracted from the cultured cells on the films using the TRIzol reagent (Invitrogen, San Diego, CA) according to the manufacturer's recommended protocol. Following DNAseI treatment, reverse transcription of 0.5 mg of total RNA was performed using MMLV reverse transcriptase (Clontech, Carlsbad, CA) in the presence of oligo (dT) primers (Clontech). The type I collagen (Col) and osteocalcin (OC) mRNA were detected using the primer designs, annealing temperature and cycle numbers determined previously previously[32]. PCR products were visualized on 1.5 % agarose gel by ethidium bromide staining. Band intensity was detected and quantified under UV light and normalized to GAPDH mRNA.

2.8 Quantification of mineralization

The cells cultured on the films were stained with alizarin red S after 21 days according to a previous method[33]. In brief, the cells were fixed with cold methanol for 10 min and washed with deionized water prior to immersion for 5 min in 370 µL of 1 % Alizarin Red S (Sigma) solution dissolved in a 1:100 (v/v) ammonium hydroxide/water mixture. Each stained specimen was washed several times with deionized water to remove non-specific bonding, and it was then dissolved under 10 mmol/L sodium phosphate with 10 % cetylpyridinium chloride for 15 min, followed by spectrophotometric measurement with the absorbance at 562 nm.

2.9 Statistical analysis

All values are expressed as mean ± standard deviation. Statistical analyses were carried out by analysis of variance (one-way ANOVA) and Scheffe's post hoc test with software (SPSS Inc, SPSS 16.0) for multiple comparision tests.

3. Results

3.1 Sample fabrication and characterization

The morphological changes of the TiO_2 nanorod films with MBG incorporation are shown in Fig. 1. The cross sections of the films (Fig. 1 insert) showed that the MBG tightly cohered with TiO_2 nanorods and the substrates, keeping the density of nanorods unchanged. However, the exposed nanorod height strongly depended on MBG precursor sol concentration, and the height changed from ~300 nm (un-incorporated) to ~200 nm (0.32 M) and ~100 nm (0.4 M), designated as 300-NR, 200-NR and 100-NR films respectively.

We chose 200-NR film as the representative to detect the element distribution in single nanorod via TEM mapping analysis (Fig. 2). The shape of the nanorods was shown in Fig. 2a, the elements of Ti and O were found mainly in whole nanorods (Fig. 2b and 2c), and the element of Si appeared on the nanorods (Fig. 2d). MBG was mainly located on the surface of TiO_2 nanorods.

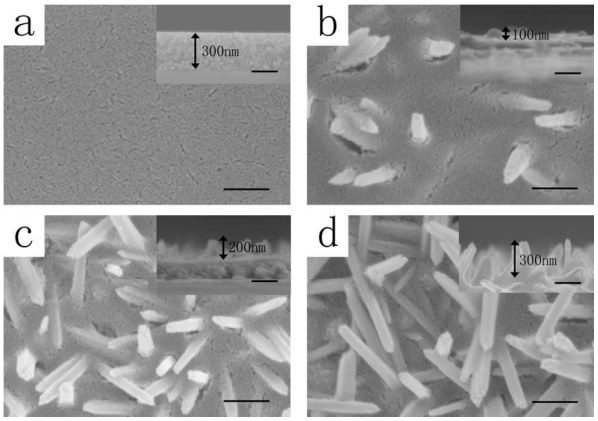

Fig. 1 SEM images (scale bar = 200 nm) and cross-section images (scale bar = 200 nm) of MBG/TiO_2 nanorod films: (a) MBG; (b)100-NR films; (c) 200-NR films; (d) 300-NR films.

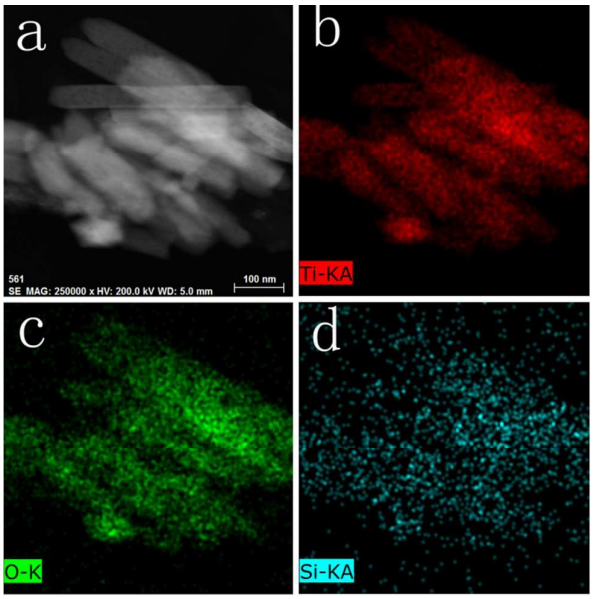

Fig. 2 TEM analysis of 200-NR films: (a) morphology of 200-NR-films; (b), (c), (d) Mapping of Ti O and Si in selected area of (a).

To reveal the wettability of different films, water contact angle measurement was conducted (Fig. 3). The contact angle of TiO_2 nanorod film (300-NR) was super hydrophilic surfaces with a contact angle around 8.5° while MBG film exerted a contact angle about 33.4°. Reasonably, the hydrophilic of 100-NR films and 200-NR films were between the two films above, respectively 25.8° and 22.2°. The incorporated films showed less hydrophilic with the increasing amount of MBG.

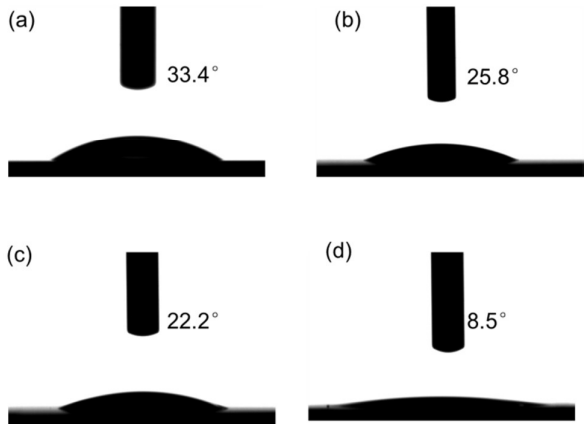

Fig. 3 Water contact angle images of different films: (a) MBG; (b)100-NR films; (c) 200-NR films; (d) 300-NR films.

3.2 Cellular attachment and proliferation

To examine the initial cellular attachment and proliferation, a short-time cell culture[25] for 1 and 3 days was carried out. The CCK-8 assay (Fig. 4) for 1 and 3 days showed that TiO_2 nanorod films had higher cell numbers than MBG films. For TiO_2 nanorod films, the films with shortened nanorod-height (100-NR and 200-NR films) showed better cell attachment than 300-NR films. After culturing for 3 days, the cell number increased, and cells on 100-NR films had faster cellular growth rate.

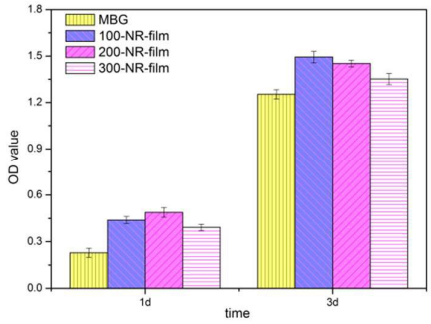

Fig.4 CCK-8 characterization of MSCs cells adhesion and proliferation on different samples

After 24-hour incubation, the filopodia morphology of MSCs were observed by SEM. More cellular filopodia with a higher degree of extension presented on 100-NR films in comparison with the cells cultured on 200-NR, 300-NR and MBG films (Fig. 5).

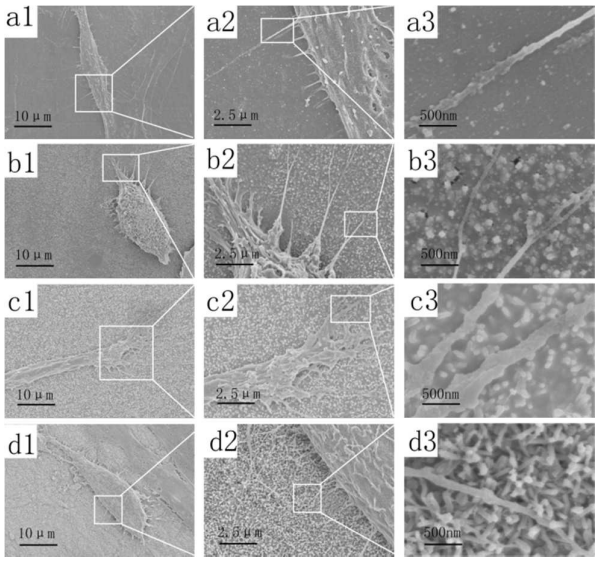

Fig. 5 SEM images of morphology of MSCs after culturing on different samples surfaces for 1 day. (a1-a3) MBG films; (b1-b3) 100-NR films; (c1-c3) 200-NR films; (d1-d3) 300-NR films.

The filopodia on the films with the shortened TiO_2 nanorod-heights could spread on both nanorods tops and bottom elevated by MBG (Fig. 5a and 5b), while the filopodia on 300-NR or MBG films only spread on the top of nanorods or MBG surface (Fig. 5c and 5e).

3.3 Cellular differentiation

ALP activity is usually assessed as an indicator of initial differentiation. The ALP activities of the cultured MSCs on the TiO_2 nanorod films were significantly stronger than those on MBG films at 7 days, and the difference became small at 14 days (Fig. 6a). For TiO_2 nanorod films, the films with shortened nanorod-height (100-NR and 200-NR films) had higher ALP activity than 300-NR films, especially, 100-NR films had significantly higher ALP activity at 7 days than others.

Collagen I and OC expressions of cultured cells are respectively considered as an early-stage marker and a late-stage marker for osteogenic tendency. The 7-day cultured cells on 100-NR and 200-NR films showed higher expression in both Col and OC than those on 300-NR films and MBG films (Fig. 6b and 6c). For the Col and OC expressions of 14-day cultured cells, the expression on TiO_2 nanorod films became much weaker for Col and decreased for OC, however, the expression on MBG films became stronger for Co1 and nearly remained unchanged for OC.

Journal Name

ARTICLE

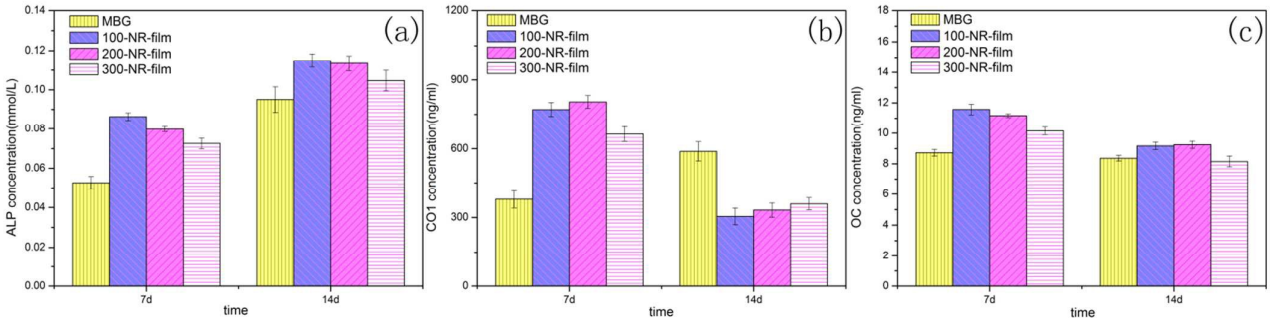

Fig. 6 (a) ALP activity expression (b) Co1 expression (c) OC expression of MSCs on different samples

P-smads level is used to estimate the intension of effects on promoting osteogenic differentiation by BMP-smads signal pathway. Smad1/5/8 is a key protein involved in the BMP-signaling pathway, subsequent regulating the osteogenic genes[26]. The P-smads levels of the 7-day cultured MSCs on TiO_2 nanorod films were higher than that on MBG films, and 100-NR films showed the significantly strongest effect (Fig. 7).

Based on the Fig. 6, 100-NR films demonstrated to provide MSCs with stronger activity in the early stage of osteogenic differentiation. The higher P-smads levels for 100-NR and 200-NR films (Fig. 7) demonstrated the shortening of nanorod-heights could let the surface approach to a cellular recognition microenvironment and strengthen BMP-smads signal pathway.

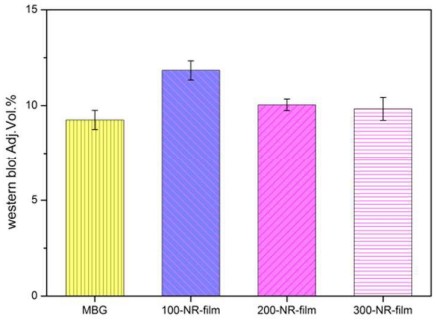

Fig. 7 Smad 1/5/8 phosphorylation degree of MSCs after culturing on different samples for 7 days.

3.4 Cellular mineralization

As indicator of late stage osteogenesis, cellular mineralization at 21 days was assessed. Alizarin red staining was employed to evaluate mineralization. After culturing MSCs for 21 days, the result (Fig. 8) showed that 100-NR films behaved the best in cellular mineralization, the next 200-NR films, and 300-NR films had higher mineralization degrees than MBG films. It is a reasonable subsequence for the well-conditioned cells at early stage.

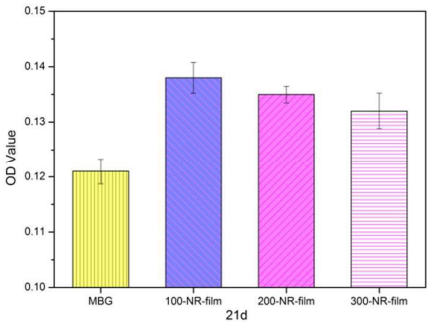

Fig. 8 Quantitive result of mineralization of MSCs through alizarin red staining after culturing on different samples for 21 days.

4. Discussion

When MBG was incorporated into TiO_2 nanorod films, the exposed nanorod-height in the films was successfully adjusted from original ~300 nm to ~200 nm and ~100 nm, along with unchanged nanorod-density (Fig. 1). The films with shortened nanorod-heights (100-NR and 200-NR films) showed an obvious difference in cellular responses from the original film (300-NR film). The results of elements mapping in Fig. 2 suggest that incorporated MBG tightly bonded with TiO_2 nanorods, which demonstrates the stability of film structure. Besides, the films tested were all hydrophilic, and the incorporated films showed less hydrophilic with the increasing amount of MBG (Fig. 3).

For cell adhesion and proliferation, 100-NR and 200-NR films had better cellular responses than 300-NR films (Fig. 4), MBG films, showing least filopodia extension and lowest proliferation for cell culturing both 1 day and 3 days. This illustrates that the three-dimension nanostructure of nanorods benefits the cells attachment and proliferation (Fig. 5). What is more, the shortened nanorods of 100-NR and 200-NR films provided an optimal height to support the cells spread along both the top of nanorods and MBG surfaces, leading to more intensified interaction with the microenvironment. These results are coincidence with our previous work that higher cellular proliferation of the cultured cells on 180 nm-height nanorods rather than 410 nm-height nanorods[27]. It can be speculated that the 100-NR and 200-NR films offer an appropriate range of three-dimension nanostructure for cellular recognition, thus contribute to enhanced dynamic propagation and an increase in MSCs activation, as indicated by the filopodia.

MSCs on the TiO_2 nanorod films had stronger osteogenic differentiation activity than MBG films (Fig. 6), and 100-NR and 200-NR films had tendencies of increasing ALP activity of cells, and decreasing Col and OC expressions with culture period from 7th day to 14th day. This elucidates that the MSCs on these films had stronger osteogenic differentiation activity at early stage (7 days), and had begun to enter into the core differentiation period and developed almost to osteoblasts after 7 days, thus Col and OC expressions after 14 days would drop.

It has already been revealed that the increased p-Smad1/5/8 greatly activated the BMP signal pathway, which accelerated the osteogenic differentiation of MSCs[25]. Here, the higher p-smads levels for 100-NR and 200-NR films (Fig. 7) again demonstrated the shortening of nanorod-heights could let the surface approach to a cellular recognition microenvironment and strengthen BMP-smads signal pathway. It was consistent with our above differentiation results at the gene level (Fig. 6 and Fig. 7). Furthermore, in consideration of mineralization as a longer-term result (Fig. 8), it further confirms that 100-NR films enhanced the most osteogenic differentiation of MSCs.

According to results above, we could conclude that a three-dimension nanostructure of nanorod was beneficial for promoting MSCs adhesion and proliferation, and subsequently accelerating MSCs towards to osteogenic differentiation and mineralization. Fig. 4 demonstrates that the film with ~100 nm exposed height of TiO_2 nanorods (100-NR) seems to provide an optimal three-dimension nanostructure for cellular development, such a nanostructure could be considered to exert lager contact area and more active sites for inducing more proteins including fibronectin, integrins BMPs and cellular vinculin[27], which would subsequently contribute to cell attachment and development. Besides, the filopodia of MSCs may tend to have better interactions with material surface. Filopodia tends to extend in horizontal directions instead of vertical directions according to Fig. 4 and other reports[28]. Thus original nanorod structure is too high for the cells to sense the bottom of nanostructure. A shortened height of nanorods like 100-NR films makes filopodia easier to touch the bottom of the nanostructure.

Hence, a nanostructure with highly biological responses depends on not only the selection of geometrical units in materials and shapes, but also the topologic arrangement of the units. The precise underlying mechanisms of the cell-materials interactions need to be further investigated because the interactions are sophisticated.

5. Conclusions

The exposed nanorod-heights of TiO_2 nanorod films were adjusted from original ~300 nm to ~200 nm and ~100 nm with MBG incorporation via sol-gel spin-coating. Based on the culture results of MSCs, the films with shortened nanorod-heights showed to enhance cellular responses and could accelerate osteogenic differentiation and mineralization. Comprehensively, the films with 100 nm nanorod-height demonstrated the best niche for cell growth. The reason is suggested that the films with the shortened nanorod-heights could provide a more cellular recognizable microenvironment to enhance the interactions with cells, prompting the cells to develop faster towards to the stage of osteogenic differentiation due to strengthening BMP-smads signal pathway. This work endeavours to provide deeper insight for understanding the cell-material interactions. It could be helpful for our understanding of the role of nanostructures in accelerating osteogenesis, and the present approach might be a promising way of surface modification for orthopedic metal implants.

Acknowledgements

This work is financially supported by the National Natural Science Foundation of China (51272228, 81271955, 51472216, 51372217), National Basic Research Program of China (973 Program, 2012CB933600). The Key Science Technology Innovation Team of Zhejiang Province (2013TD02), Natural Science Foundation of Zhejiang (LY15E020004) and Fundamental Research Funds for the Central Universities (2013QNA4010, 2014XZZX005).

References

1. L. Xia, N. Zhang, X. Wang, Y. Zhou, L. Mao, J. Liu, X. Jiang, Z. Zhang, J. Chang, K. Lin and B. Fang, *J. Mater. Chem. B*, 2016, **4**, 3313-3323.
2. J. Feng, Z. Wang, B. Shen, L. Zhang, X. Yang and N. He, *RSC Advances*, 2014, **4**, 28683.

3. T. U. Luu, S. C. Gott, B. W. Woo, M. P. Rao and W. F. Liu, *ACS applied materials & interfaces*, 2015, **7**, 28665-28672.
4. W. A. El-Said, C. H. Yea, M. Jung, H. Kim and J. W. Choi, *Ultramicroscopy*, 2010, **110**, 676-681.
5. J. Park, S. Bauer, A. Pittrof, M. S. Killian, P. Schmuki and K. von der Mark, *Small*, 2012, **8**, 98-107.
6. J. Song, G. Fu, Q. Cheng and Y. Jin, *Industrial & Engineering Chemistry Research*, 2014, **53**, 708-714.
7. S. Bagherifard, R. Gheichi, A. Khademhosseini and M. Guagliano, *ACS applied materials & interfaces*, 2014, **6**, 7963-7985.
8. G. Li, H. Cao, W. Zhang, X. Ding, G. Yang, Y. Qiao, X. Liu and X. Jiang, *ACS applied materials & interfaces*, 2016, **8**, 3840-3852.
9. K. Kubo, N. Tsukimura, F. Iwasa, T. Ueno, L. Saruwatari, H. Aita, W. A. Chiou and T. Ogawa, *Biomaterials*, 2009, **30**, 5319-5329.
10. H. Zhao, W. Dong, Y. Zheng, A. Liu, J. Yao, C. Li, W. Tang, B. Chen, G. Wang and Z. Shi, *Biomaterials*, 2011, **32**, 5837-5846.
11. J. J. Khandare, A. Jalota-Badhwar, S. D. Satavalekar, S. G. Bhansali, N. D. Aher, F. Kharas and S. S. Banerjee, *Nanoscale*, 2012, **4**, 837-844.
12. X. W. Liu, D. X. Wei, J. Zhong, M. J. Ma, J. Zhou, X. T. Peng, Y. Ye, G. Sun and D. N. He, *ACS applied materials & interfaces*, 2015, **7**, 18540-18552.
13. J. Zhou, B. Li, S. Lu, L. Zhang and Y. Han, *ACS applied materials & interfaces*, 2013, **5**, 5358-5365.
14. D. Zhao, G. Wang, Z. He, H. Wang, Q. Zhang and Y. Li, *J. Mater. Chem. B*, 2015, **3**, 4272-4281.
15. Z. Li, X. Lv, S. Chen, B. Wang, C. Feng, Y. Xu and H. Wang, *RSC Adv.*, 2016, **6**, 42229-42239.
16. J.-H. Seo, M. Hirata, S. Kakinoki, T. Yamaoka and N. Yui, *RSC Adv.*, 2016, **6**, 35668-35676.
17. X. Dai, X. Zhang, M. Xu, Y. Huang, B. C. Heng, X. Mo, Y. Liu, D. Wei, Y. Zhou, Y. Wei, X. Deng and X. Deng, *RSC Adv.*, 2016, **6**, 43685-43696.
18. J. Azadmanjiri, P.-Y. Wang, H. Pingle, P. Kingshott, J. Wang, V. K. Srivastava and A. Kapoor, *RSC Adv.*, 2016, DOI: 10.1039/c6ra10289a.
19. T.-H. Chung, C.-C. Hsieh, J.-K. Hsiao, S.-C. Hsu, M. Yao and D.-M. Huang, *RSC Adv.*, 2016, **6**, 45553-45561.
20. M. Li, F. Zhang, K. Chen, C. Wang, Y. Su, Y. Liu, J. Zhou and W. Wang, *RSC Adv.*, 2016, **6**, 36910-36922.
21. D. Tang, K. Cheng, W. Weng, C. Song, P. Du, G. Shen and G. Han, *Thin Solid Films*, 2011, **519**, 7644-7649.
22. M. Luo, K. Cheng, W. Weng, C. Song, P. Du, G. Shen, G. Xu and G. Han, *Nanotechnology*, 2009, **20**, 215605.
23. H. J. Zheng, J. A. Martin, Y. Duwayri, G. Falcon and J. A. Buckwalter, *Journals of Gerontology Series a-Biological Sciences and Medical Sciences*, 2007, **62**, 136-148.
24. Y. Vida, D. Collado, F. Najera, S. Claros, J. Becerra, J. A. Andrades and E. Perez-Inestrosa, *RSC Adv.*, 2016, **6**, 49839-49844.
25. D. D. Liu, K. Ge, J. Sun, S. Z. Chen, G. Jia and J. C. Zhang, *Rsc Advances*, 2015, **5**, 42233-42241.
26. D. Liu, K. Ge, J. Sun, S. Chen, G. Jia and J. Zhang, *RSC Adv.*, 2015, **5**, 42233-42241.
27. K. Cheng, M. Yu, Y. Liu, F. Ge, J. Lin, W. Weng and H. Wang, *Colloids and surfaces. B, Biointerfaces*, 2015, **126**, 387-393.
28. P. Y. Collart-Dutilleul, I. Panayotov, E. Secret, F. Cunin, C. Gergely, F. Cuisinier and M. Martin, *Nanoscale Research Letters*, 2014, **9**, 10.

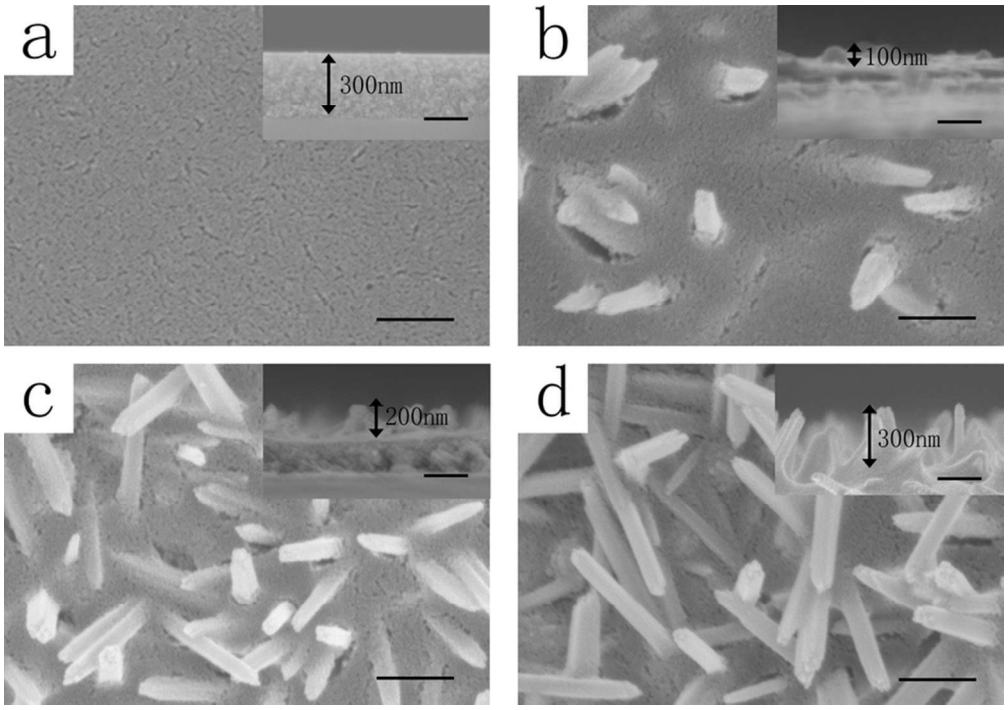

77x54mm (300 x 300 DPI)